Tetrahedron 75 (2019) 912–920

Contents lists available at ScienceDirect

Tetrahedron

journal homepage: www.elsevier.com/locate/tet

A novel donor-π-acceptor anthracene monomer: Towards faster and milder reversible dimerization

Jonas Van Damme [a], Otto van den Berg [a, b], Joost Brancart [b], Guy Van Assche [b], Filip Du Prez [a, *]

[a] Polymer Chemistry Research Group, Centre of Macromolecular Chemistry (CMaC), Department of Organic and Macromolecular Chemistry, Faculty of Sciences, Ghent University, Krijgslaan 281, S4-bis, B-9000 Ghent, Belgium
[b] Research Unit of Physical Chemistry and Polymer Science (FYSC), Vrije Universiteit Brussel (VUB), Pleinlaan 2, B-1050 Brussels, Belgium

ARTICLE INFO

Article history:
Received 7 November 2018
Received in revised form
4 January 2019
Accepted 5 January 2019
Available online 7 January 2019

Keywords:
Anthracene derivatives
2,6-Substituted
Dimerization
Scission

ABSTRACT

A novel functional 2,6-substituted donor-acceptor anthracene derivative, bearing a long alkyl spacer and a polymerizable end-group, is synthesized from readily available compounds. This monomer possesses conjugated electron donor and acceptor moieties to achieve UV absorption and anthracene dimerization at higher wavelengths and under milder conditions, than anthracene and other reported anthracene derivatives. The compound was shown to absorb at higher wavelengths and dimerize much faster compared to most 9-substituted anthracenes. The fast photochemical and relatively slow thermal scission of the dimers were studied and related to the chemical structure, *i.e.* the 2,6-substitution.

1. Introduction

One of the most interesting properties of anthracene and anthracene derivatives is their reversible dimerization, which occurs via a [4 + 4]-cycloaddition upon exposure to UV-light [1]. Subsequent scission of the formed dimers is known to occur not only photochemically, but also thermally and mechanically [2]. Because of these properties, their potential applications as molecular switches [3], mechanophores [4], anti-counterfeit polymers [5] and reversibly cyclized crown ethers [6,7] have been studied.

Over the past decades, reversible covalent bonds have made their way into polymer science for many applications such as self-healing materials, recyclable polymers and stress-relaxing materials [8–13]. Many reviews discuss the use of these reversible chemistries in polymer science, which can be classified into additive or exchange-type reactions and dissociative reactions [8–18]. The additive reactions rely on a dynamic exchange of reversible bonds, without a net change in the number of bonds formed. Examples hereof are transesterifications, transamidations and trithiocarbonate reshuffling [19,20]. Dissociative chemistries occur by scission of bonds, followed by the formation of bonds. Well-known examples of these reactions are thermoreversible Diels-Alder [4 + 2] cycloadditions between dienes and dienophiles, and photoreversible dimerizations of coumarines, cinnamates and anthracene [17,21–23]. The thermoreversible addition reactions rely on a thermal equilibrium between the bond-forming and bond-breaking reactions, while the photoreversible dimerization reactions are characterized by an ON/OFF type of reaction kinetics, where the bond-forming and bond-breaking stimuli can be applied either separately or simultaneously. More information on anthracene containing polymers can be found in our recent review [24].

The fact that the number of publications on anthracene as photoreversible bond in polymers is limited could be ascribed to the limited availability of functional derivatives [24–26]. In fact, the majority of publications use 9-substituted derivatives (Scheme 1), many of which are based on 9-anthracenemethanol [27]. Recently, we developed several functional 9-substituted anthracene derivatives and evaluated their properties for use in polymer materials [28]. It was shown how different substituents heavily influence the thermal scission. One of these derivatives was then subsequently used to develop remendable thiol-ene elastomers [29]. In another recent study, Barner-Kowollik, Delaittre and coworkers used a novel strongly electron-donating 9-substituent to allow the reversible dimerization to occur at higher wavelengths

* Corresponding author.
E-mail address: filip.duprez@ugent.be (F. Du Prez).

https://doi.org/10.1016/j.tet.2019.01.007
0040-4020/

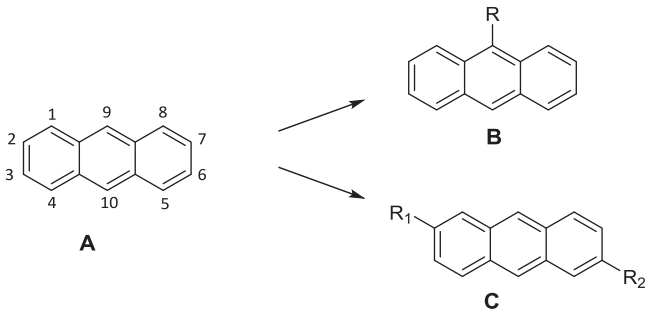

Scheme 1. Representation of anthracene (A), 9-substituted- (B) and 2,6-substituted-anthracene derivatives (C) (with R, R_1, R_2 being random functional groups).

[30]. In a publication by Yamamoto and coworkers concerning reversible cyclization, several 9-substituted derivatives were evaluated to enhance the photo-oxidative stability of the anthracene moieties [31].

In the endeavor to have a large impact on the photodimerization properties, we aimed to develop functional 2,6-substituted anthracenes (Scheme 1). The absence of a substituent on the central ring is known to improve the dimerization rate by reducing steric hindrance. Furthermore, we favored to have two different substituents with the assumption that this will lead to a shift of the absorption to (much) higher wavelengths because of a synergetic effect of the conjugated donor acceptor units. These shifts in absorption and fluorescence in donor-π-acceptor anthracenes have previously been demonstrated by Lu et al. [32] and Ihmels [33]. Initially, inspired by their publications, we aimed to develop a new upscalable synthetic pathway to create donor-π-acceptor anthracenes from readily available compounds with the possibility to obtain useful derivatives by small synthetic changes. One of the resulting derivatives contains an alkyl chain to improve its solubility and can be incorporated as (di)anthracene monomer in existing polymer formulations. The absorption, dimerization and scission properties of this derivative has been studied, related to its structure and evaluated in the context of reversible bond formation in polymers and polymer materials.

2. Experimental

2.1. Materials & methods

All chemicals were purchased from either Acros Organics, Sigma-Aldrich or TCI Europe and used as such. IR spectra were recorded using a Perkin Elmer FTIR SPECTRUM 1000 equipped with a PIKE Miracle ATR unit. NMR spectra were recorded with a Bruker Avance-III (400 MHz) NMR spectrometer. Differential scanning calorimetry (DSC) was performed using a DSC1/700 Mettler-Toledo apparatus. The used heating rate was 10 K min^{-1} and all measurements were done under nitrogen flow. This technique was also used to study the bulk thermal scission behavior of the dimer. Melting points were determined using the IA90000 melting point apparatus from Electrothermal at a heating rate of 1 K min^{-1}. LC-MS analyses were performed on an Agilent Technologies 1100 series LC/MSD system with a diode array detector (DAD) and single quad MS. Analytical reversed phase HPLC analyses were performed with a Phenomenex Luna C18 (2) column (5 μm, 250 mm × 4.6 mm) and a solvent gradient (75–100% acetonitrile in H_2O in 15 min), the eluted compounds were analyzed via UV detection (214 nm). UV dimerization occurred under inert atmosphere in a Metalight Classic from Primotec, with 12 double 365 nm UV lamps of 9 W each (intensity measured in the middle ~ 5 mW cm^{-2}). For fluorescence analysis, a Cary Eclipse Fluorescence Spectrophotometer from Agilent with a Xenon flash lamp was used. Excitation occurred at the absorption peak maxima in the 350–400 nm region and the fluorescence spectrum was measured between up to 600 nm with a 2.5 nm slit and a scan rate of 600 nm min^{-1}. UV–vis absorption was measured using a Specord 200 from AnalyticJena from 200 to 600 nm with a speed of 5 nm s^{-1}, a slit of 2 nm and $\Delta\lambda = 0.1$ nm. For quantum yield determinations, the concentration of the samples was chosen to ensure a transmission of 90–99% at the emission wavelength. 9,10-Diphenylanthracene in ethanol ($\Phi_f = 0.95$) was used as standard in the quantum yield calculations using following equation,

$$\Phi = \Phi_R \frac{Int}{Int_R} \frac{1 - 10^{-A_R}}{1 - 10^{-A}} \frac{\eta^2}{\eta_R^2}$$

where "*Int*" is the integrated area under the fluorescence curve, *A* the absorption, η the refractive index of the medium and Φ the fluorescence quantum yield. Subscript "*R*" is used when referring to the standard. The uncertainty on the activation energies and pre-exponential factor was determined using Excel's LINEST function.

2.2. Synthesis

2.2.1. Synthesis of 2-Bromo-5-methoxybenzaldehyde (**2**)

To a stirring solution of *m*-anisaldehyde (100 mL, 0.82 mol, 1 equiv.) in acetic acid (300 mL), bromine (50 mL, 0.97 mol, 1.2 equiv.) was slowly added over 30 min. The solution was stirred without additional heating for 2 h, followed by 1 h heating at 70 °C. The reaction mixture was added to water (1.5 L), resulting in an orange precipitation. After filtration, the solids were washed with water and a bicarbonate solution. The crude product was recrystallized in hot ethanol, resulting in 2-bromo-5-methoxybenzaldehyde **2** as an off-white solid (123 g, 0.57 mol, 70% yield). To recuperate the remaining product dissolved in ethanol, a sodium hydrogen sulfite solution (37.5%, 250 mL) was added. The formed salts were filtered and washed with ethanol and water. These salts were dissolved in a minimal amount of hot acetic acid. After cooling, bromo-5-methoxybenzaldehyde **2** crystallized out of solution (36 g, 0.17 mol, 21% yield, Figs. S1–S3). Total yield was 91%; *mp* = 73.5–75 °C; ^{1}H NMR (400 MHz, $CDCl_3$): δ (ppm) = 3.85 (s, 3H, OCH_3), 7.04 (dd, 1H, *J* = 8.8 Hz, *J* = 3.3 Hz, CCHCHCBr), 7.43 (d, 1H, *J* = 3.2 Hz, CCHC), 7.53 (d, 1H, *J* = 8.8 Hz, CCHCHCBr), 10.32 (s, 1H, CHO); ^{13}C NMR (100 MHz, $CDCl_3$): δ (ppm) = 55.7 (CH_3), 112.7 (CH), 118 (C), 123.1 (CH), 134 (C), 134.6 (CH), 159.3 (C), 181.8 (CH); IR ν_{max} cm^{-1}: 3006, 2942, 2874, 2744, 2031, 1896, 1676, 1569, 1467, 1278, 1198, 1060, 1012; GC-MS (*m/z*) 214 $[M]^+$; not detectable in LC-MS.

2.2.2. Synthesis of (2-Bromo-5-methoxyphenyl)(4-chlorophenyl) methanol (**4**)

Magnesium flakes (14.4 g, 592 mmol, 1.65 equiv.) were crushed and placed in a flame-dried two-neck flask equipped with a reflux cooler under inert atmosphere. Bromine (0.3 mL, 5.8 mmol) was added to the magnesium flakes. The flask was stirred and heated to the boiling point of the bromine for 15 min and afterwards cooled using an ice bath. Anhydrous diethyl ether (60 mL) was quickly added. The ice bath was removed. A solution of 1-bromo-4-chlorobenzene (74.5 g, 394 mmol, 1.1 equiv.) in anhydrous diethyl ether (120 mL) was slowly added at a rate which kept the exothermic reaction at reflux conditions. This solution was stirred for 1 h at room temperature, after which a solution of 2-bromo-5-methoxybenzaldehyde **2** (77 g, 358 mmol, 1 equiv.) in anhydrous diethyl ether (320 mL) was slowly added. After all aldehyde was added, the mixture was stirred for 1 h at room temperature. The

reaction mixture was carefully poured in a 1 M HCl solution (1 L). The organic phase was separated and combined with diethyl ether washings of the aqueous phase (2 × 100 mL). After drying using sodium sulfate, the organic fractions were concentrated *in vacuo*. This crude liquid (2-bromo-5-methoxyphenyl)(4-chlorophenyl) methanol **4** (120 g) was used as such in the next step. For analytical characterization (Figs. S4–S6), a small amount was purified using column chromatography (eluents: hexane:ethyl acetate). ^{1}H NMR (400 MHz, $CDCl_3$): δ (ppm) = 2.38 (d, 1H, J = 3.8 Hz, CHOH), 3.80 (s, 3H, OCH_3), 6.13 (d, 1H, J = 3.8 Hz, CHOH), 6.74 (dd, 1H, J = 8.7 Hz, J = 3.1 Hz, CCHCHCBr), 7.12 (d, 1H, J = 3.1 Hz, CCHC), 7.29–7.38 (m, 4H, CCHCHCCl), 7.43 (d, 1H, J = 8.8 Hz, CCHCHCBr); ^{13}C NMR (100 MHz, $CDCl_3$): δ (ppm) = 55.5 (CH_3), 74.1 (CH), 112.8 (C), 113.9 (CH), 115.1 (CH), 128.4 (CH), 128.6 (CH), 133.5 (CH), 133.6 (C), 140.4 (C), 143.1 (C), 159.3 (C); IR ν_{max} cm^{-1}: 3730, 3625, 3584, 3002, 2936, 2836, 2360, 1594, 1469, 1417, 1291, 1236, 1159, 1130, 1090, 1049, 1013; LC-MS (*m/z*) 309.0 [M-OH]$^+$; HRMS (*m/z* for [M-OH]$^+$) calcd.: 308.9682; found: 308.9673.

2.2.3. Synthesis of 1-Bromo-2-(4-chlorobenzyl)-4-methoxybenzene (*5*)

Crude (2-bromo-5-methoxyphenyl)(4-chlorophenyl)methanol **4** (120 g, theoretically 358 mmol, 1 equiv.) was dissolved with triethyl silane (57.5 mL, 360 mmol, 1 equiv.) in dichloromethane (500 mL). While this solution stirred, trifluoroacetic acid was slowly added (250 mL). The reaction was stirred for 18 h at room temperature. The reaction mixture was concentrated *in vacuo* and purified via column chromatography (hexane:ethyl acetate 95:5). This yielded the pure 1-bromo-2-(4-chlorobenzyl)-4-methoxybenzene **5** as a colorless liquid (103 g, 331 mmol, 92% yield, Figs. S7–S9). ^{1}H NMR (400 MHz, $CDCl_3$): δ (ppm) = 3.76 (s, 3H, OCH_3), 4.05 (s, 2H, CH_2), 6.67–6.71 (m, 2H, CCHC + CCHCHCBr), 7.12–7.17 (m, 2H, CCHCHCl), 7.26–7.30 (m, 2H, CCHCHCl), 7.44–7.50 (m, 1H, CCHCHCBr); ^{13}C NMR (100 MHz, $CDCl_3$): δ (ppm) = 41.2 (CH_2), 55.4 (CH_3), 113.5 (CH), 115.2 (C), 117 (CH), 128.6 (CH), 130.3 (CH), 132.1 (C), 133.4 (CH), 137.8 (C), 140.8 (C), 159 (C); IR ν_{max} cm^{-1}: 2934, 2834, 1894, 1572, 1471, 1238, 1158, 1089; GC-MS (*m/z*) 310 [M]$^+$

2.2.4. Synthesis of 2-(4-Chlorobenzyl)-4-methoxybenzoic acid (*6*)

Magnesium flakes (4.7 g, 193 mmol, 1.5 equiv.) were crushed and placed in a flame-dried two-neck flask equipped with a reflux cooler under inert atmosphere. Anhydrous tetrahydrofuran (20 mL) was added to the flask, followed by a small iodine crystal. While this mixture stirred, a solution of 1-bromo-2-(4-chlorobenzyl)-4-methoxybenzene **5** (40 g, 128 mmol, 1 equiv.) in anhydrous tetrahydrofuran (80 mL) was prepared. This solution of **5** was carefully added to the magnesium over 1 h while maintaining reflux conditions using external heating. The mixture was left to stir for another 45 min at room temperature. Dried CO_2 gas was slowly added to the atmosphere just above the solution surface using a syringe, while heavily stirring the solution. This resulted in an exothermic response. This CO_2 originated from subliming dry ice and the formed gas was dried by bubbling twice through concentrated sulfuric acid before it reached the reaction mixture. After 1 h, the solution had cooled down and the CO_2 flush was stopped. The reaction mixture was stirred for another 40 h under CO_2 atmosphere. The reaction mixture was poured in dilute HCl solution (1 M, 400 mL). The yellow precipitate was filtered off and dissolved in a dilute NaOH solution (1 M, 400 mL). Concentrated HCl solution (12 M) was added to the basic solution to a pH of approximately 2. The precipitated solid was filtered off and dried, rendering pure 2-(4-chlorobenzyl)-4-methoxybenzoic acid **6** (31 g, 113 mmol, 88%, Figs. S10–S12); *mp* = 144–155 °C; ^{1}H NMR (400 MHz, DMSO-d_6): δ (ppm) = 3.78 (s, 3H, OCH_3), 4.35 (s, 2H, CH_2), 6.85 (d, 1H, J = 2.6 Hz, CCHC), 6.89 (dd, 1H, J = 8.7, J = 2.7 Hz, CCHCHCCO), 7.14–7.19 (m, 2H, CCHCHCCl), 7.27–7.32 (m, 2H, CCHCHCCl), 7.87 (d, 1H, J = 8.67 Hz, CCHCHCCO); ^{13}C NMR (100 MHz, DMSO-d_6): δ (ppm) = 38.1 (CH_2), 55.3 (CH_3), 111.5 (CH), 117.2 (CH), 122.0 (C), 128.1 (CH), 130.4 (CH), 132.7 (C), 133.2 (CH), 140.2 (C), 144.1 (C), 161.9 (C), 167.9 (C); IR ν_{max} cm^{-1}: 3000, 2937, 2836, 2637, 2560, 2361, 2173, 2027, 1682, 1601, 1487, 1406, 1244, 1148, 1078, 1032; LC-MS (*m/z*) 275.1 [M-H]$^-$; HRMS (*m/z* for [M-H]$^-$) calcd.: 275.0475; found: 275.0487.

2.2.5. Synthesis of 2-Chloro-6-methoxyanthracen-9(10H)-one (*7*)

2-(4-chlorobenzyl)-4-methoxybenzoic acid **6** (18.35 g, 66.3 mmol, 1 equiv.) was added to thionyl chloride (200 mL). After adding a catalytic amount of dimethyl formamide, this reaction mixture was heated to reflux conditions for 2 h. The formed acid chloride was concentrated *in vacuo*. Anhydrous dichloromethane was added, followed by aluminum trichloride (13.3 g, 99.8 mmol, 1.5 equiv.). After 1 h of stirring at room temperature, the reaction mixture was poured on ice. When this mixture reached room temperature, the organic phase was separated from the aqueous phase. The aqueous phase was extracted with chloroform (2 × 100 mL). The combined organic fractions were dried using sodium sulfate and concentrated *in vacuo* to give 2-chloro-6-methoxyanthracen-9(10*H*)-one **7** as a brown solid (17.1 g, 66.1 mmol, 100%, Figs. S13–S15); *mp* = 162–165.5 °C; ^{1}H NMR (400 MHz, $CDCl_3$): δ (ppm) = 3.91 (s, 3H, OCH_3), 4.27 (s, 2H, CH_2), 6.89 (s, 1H, CCHCOCH$_3$), 7.00 (dd, 1H, J = 8.8 Hz, J = 2.1 Hz, CCHCHCOCH$_3$), 7.38 (d, 1H, J = 8.3 Hz, CCHCHCCl), 7.51 (dd, 1H, J = 8.2 Hz, J = 2.1 Hz, CCHCHCCl), 8.27–8.35 (m, 2H, CCHCCl + CCHCHCOCH$_3$); ^{13}C NMR (100 MHz, $CDCl_3$): δ (ppm) = 32.1 (CH_2), 55.5 (CH_3), 111.9 (CH), 114.4 (CH), 125.2 (C), 127.1 (CH), 129.8 (CH), 130.1 (CH), 132.4 (CH), 133.2 (C), 133.4 (C), 138.4 (C), 142.6 (C), 163.4 (C), 182.0 (C); IR ν_{max} cm^{-1}: 3064, 2942, 2840, 2033, 1591, 1478, 1408, 1272, 1167, 1113, 1030; LC-MS (*m/z*) 259.0 [M+H]$^+$; HRMS (*m/z* for [M]$^+$) calcd.: 258.0448; found: 258.0443.

2.2.6. Synthesis of 2-Chloro-6-methoxyanthracene (*8*)

2-Chloro-6-methoxyanthracen-9(10*H*)-one **7** (18.4 g, 71.1 mmol, 1 equiv.) was dissolved in diglyme (350 mL). To this solution, sodium borohydride (18.0 g, 476 mmol, 6.7 equiv.) was added, which made the solution color turn to dark red. The solution was stirred for 30 min at room temperature. The reaction flask was placed in an ice bath and anhydrous methanol (360 mL) was slowly added over 45 min. This resulted in gas formation and disappearance of the red color. After another 15 min, more sodium borohydride (9.0 g, 238 mmol, 3.3 equiv.) was slowly added, causing additional gas formation. The reaction mixture was stirred overnight at room temperature. To the reaction mixture, acetic acid (700 mL) was added, followed by concentrated HCl solution (12 M, 100 mL). This mixture was stirred for 2 h. Water (3 L) was added to the reaction mixture, resulting in the precipitation of 2-chloro-6-methoxyanthracene **8** as a yellow solid (16.9 g, 69.6 mmol, 98%, Figs. S16–S18); *mp* = 213–214 °C; ^{1}H NMR (400 MHz, $CDCl_3$): δ (ppm) = 3.98 (s, 3H, OCH_3), 7.16–7.24 (m, 2H, CCHCHCO + CCHCO), 7.37 (dd, 1H, J = 9.0 Hz, J = 2.0 Hz, CCHCHCCl), 7.89 (d, 2H, J = 9.4 Hz, CCHCHCO + CCHCHCCl), 7.95 (d, 1H, J = 2.0 Hz, CCHCCl), 8.26 (m, 2H, CCHC); ^{13}C NMR (100 MHz, $CDCl_3$): δ (ppm) = 55.3 (CH_3), 103.6 (CH), 121.2 (CH), 124.4 (CH), 125.4 (CH), 126.4 (CH), 126.7 (CH), 128.8 (C), 129.3 (CH), 129.7 (CH), 130.0 (C), 130.2 (C), 130.4 (C), 132.8 (C), 157.4 (C); IR ν_{max} cm^{-1}: 3010, 2841,

2428, 2049, 1980, 1930, 1774 1618, 1466, 1343, 1269, 1175, 1027; GC-MS (m/z) 242 $[M]^+$

*2.2.7. Synthesis of 6-Methoxyanthracene-2-carbonitrile (**9**)*

2-Chloro-6-methoxyanthracene **8** (1.0 g, 4.1 mmol, 1 equiv.) was dissolved in *N*-methyl-2-pyrrolidone (10 mL). To this solution, copper cyanide was added (0.74 g, 8.3 mmol, 2 equiv.). The reaction mixture was heated to reflux conditions for 30 h. The mixture was then poured in a saturated bicarbonate solution (100 mL), followed by an extraction using diethyl ether (2 × 25 mL) and toluene (2 × 25 mL). The organic phases were combined, dried using sodium sulfate and concentrated *in vacuo*, rendering 6-methoxyanthracene-2-carbonitrile **9** (0.63 g, 2.7 mmol, 66%) as a yellow solid. The crude product was used as such in the next step. For characterization (Figs. S19–S21), part of the product was purified using column chromatography; mp = 184–189 °C; ^{1}H NMR (400 MHz, $CDCl_3$): δ (ppm) = 4.00 (s, 3H, OCH_3), 7.21–7.28 (m, 2H, CCHC**H**CO + CC**H**CO), 7.51 (dd, 1H, J = 8.7 Hz, J = 1.5 Hz, CCHC**H**CCN), 7.95 (d, 1H, J = 9.0 Hz, CC**H**CHCO), 8.00 (d, 1H, J = 8.8 Hz, CC**H**CHCCN), 8.30 (s, 1H, CC**H**CCHCO), 8.40 (m, 1H, CC**H**CCN), 8.42 (s, 1H, CC**H**CCHCCN); ^{13}C NMR (100 MHz, $CDCl_3$): δ (ppm) = 55.4 (CH_3), 103.6 (CH), 107.7 (C), 119.6 (C), 121.9 (CH), 124.6 (CH), 124.8 (CH), 127.8 (CH), 128.4 (C), 129.0 (CH), 130.1 (CH), 132.1 (C), 134.8 (C), 135.7 (CH), 158.6 (C); IR ν_{max} cm^{-1}: 3077, 2914, 2848, 2428, 2357, 2195, 2043, 1983, 1846, 1717, 1630, 1467, 1419, 1245, 1101, 1025; HRMS (m/z for $[M]^+$) calcd.: 233.0841; found: 233.0833.

*2.2.8. Synthesis of 6-Methoxyanthracene-2-carboxylic acid (**10**)*

6-Methoxyanthracene-2-carbonitrile **9** (0.63 g, 2.7 mmol, 1 equiv.) was added to a mixture of methanol (95 mL), water (25 mL) and potassium hydroxide (25 g). The reaction mixture was heated overnight at reflux temperature. After cooling down, water (350 mL) was added, followed by slow addition of concentrated HCl solution (50 mL). After extraction with dichloromethane (3 × 200 mL), the organic phases were combined, dried with sodium sulfate and concentrated *in vacuo*. The resulting solid was recrystallized twice in acetic acid, rendering pure 6-methoxyanthracene-2-carboxylic acid **10** as a yellow powder (0.60 g, 2.4 mmol, 87%, Figs. S22–S24); mp > 300 °C; ^{1}H NMR (400 MHz, DMSO-d_6): δ (ppm) = 3.94 (s, 3H, OCH_3), 7.25 (dd, 1H, J = 9.2 Hz, J = 2.5 Hz, CCHC**H**CO), 7.44 (d, 1H, J = 2.4 Hz, CC**H**CO), 7.90 (dd, 1H, J = 8.7 Hz, J = 1.6 Hz, CCHC**H**CCOOH), 8.05 (d, 1H, J = 9.5 Hz, CC**H**CHCO), 8.08 (d, 1H, J = 9.4 Hz, CC**H**CHCCOOH), 8.47 (s, 1H, CC**H**C), 8.72 (s, 1H, CC**H**C), 8.74 (m, 1H, CC**H**CCOOH), 12.99 (br. s, 1H, COO**H**); ^{13}C NMR (100 MHz, DMSO-d_6): δ (ppm) = 55.3 (CH_3), 103.9 (CH), 121.0 (CH), 123.9 (CH), 124.3 (CH), 126.5 (C), 127.9 (CH), 128.1 (C), 128.5 (C), 128.6 (CH), 130.1 (CH), 131.8 (CH), 132.7 (C), 134.0 (C), 157.7 (C), 167.5 (C); IR ν_{max} cm^{-1}: 2975, 2837, 2522, 2178, 2048, 1856, 1677, 1476, 1420, 1285, 1216, 1027; LC-MS (m/z) 251.1 $[M-H]^-$; HRMS (m/z for $[M-H]^-$) calcd.: 251.0708; found: 251.0712.

*2.2.9. Synthesis of Undec-10-en-1-yl 6-methoxyanthracene-2-carboxylate (**11**)*

6-Methoxyanthracene-2-carboxylic acid **10** (774 mg, 3.07 mmol, 1 equiv.) was dissolved in anhydrous dimethyl formamide (30 mL). To this solution, potassium carbonate (0.5 g, 3.65 mmol, 1.2 equiv.) and 11-bromo-1-undecene (1.4 g, 6 mmol, 2 equiv.) were added. The reaction mixture was stirred for 24 h. The reaction mixture was concentrated *in vacuo* and purified using column chromatography (hexane:ethyl acetate 95:5) to the pure undec-10-en-1-yl 6-methoxyanthracene-2-carboxylate **11** (465 mg, 1.15 mmol, 37%, Figs. S25–S27); mp = 100–102.5 °C; ^{1}H NMR (400 MHz, $CDCl_3$): δ (ppm) = 1.25–1.45 (m, 10H, $CH_2C\underline{H}_2C\underline{H}_2CH_2$), 1.46–1.55 (m, 2H, $OCH_2CH_2C\underline{H}_2$), 1.80–1.89 (m, 2H, $OCH_2C\underline{H}_2CH_2$), 2.02–2.11 (m, 2H, $CH_2C\underline{H}_2CH{=}CH_2$), 3.95 (s, 3H, $OC\underline{H}_3$), 4.41 (t, 2H, J = 6.7 Hz, $OC\underline{H}_2CH_2$), 4.93–5.06 (m, 2H, $CH_2CH{=}C\underline{H}_2$), 5.84 (ddt, 1H, J = 17.0 Hz, J = 10.3 Hz, J = 6.7 Hz, $CH_2C\underline{H}{=}CH_2$), 7.13–7.21 (m, 2H, CC**H**CO + CCHC**H**CO), 7.89 (d, 1H, J = 9.3 Hz, CC**H**CHCO), 7.93 (d, 1H, J = 8.9 Hz, CC**H**CHCCOOR), 8.00 (dd, 1H, J = 9.0 Hz, J = 1.8 Hz, CCHC**H**CCOOR), 8.22 (s, 1H, CC**H**C), 8.42 (s, 1H, CC**H**C), 8.73–8.75 (m, 1H, CC**H**CCOOR); ^{13}C NMR (100 MHz, $CDCl_3$): δ (ppm) 26.0 (CH_2), 28.8 (CH_2), 28.9 (CH_2), 29.1 (CH_2), 29.3 (CH_2), 29.4 (CH_2), 29.4 (CH_2), 33.7 (CH_2), 55.2 (CH_3), 65.1 (CH_2), 103.5 (CH), 114.1 (CH_2), 121.0 (CH), 123.9 (CH), 124.2 (CH), 126.2 (C), 127.6 (CH), 128.5 (CH), 128.9 (C), 130.0 (CH), 132.1 (CH), 133.1 (C), 134.2 (C), 139.1 (CH), 158.0 (C), 166.8 (C); IR ν_{max} cm^{-1}: 3077, 2914, 2848, 2428, 2357, 2195, 2043, 1983, 1846, 1717, 1630, 1467, 1419, 1245, 1101, 1025; LC-MS (m/z) 405.2 $[M+H]^+$; HRMS (m/z for $[M+H]^+$) calcd.: 405.2430; found: 405.2421.

*2.2.10. Synthesis of General procedure for the formation of anthracene ester dimer (**12**)*

Undec-10-en-1-yl 6-methoxyanthracene-2-carboxylate **11** (20.4 mg, 50 μmol) was dissolved in a minimal amount of hexane (10 mL) and irradiated using UVA light (365 nm; 12 × 9 W) for 1 h. The reaction mixture was concentrated *in vacuo* to render anthracene ester dimers **12** (98% pure). Recrystallization in hexane yields completely pure dimers (Figs. S28–S30); mp = 197.5–198 °C; ^{1}H NMR (400 MHz, $CDCl_3$): δ (ppm) = 1.22–1.46 (m, 24H, $CH_2C\underline{H}_2C\underline{H}_2CH_2$), 1.72 (quin, 4H, J = 7.1 Hz, $CH_2C\underline{H}_2CH_2$), 2.05 (q, 4H, J = 6.8 Hz, $CH_2C\underline{H}_2CH{=}CH_2$), 3.63 (s, 6H, $OC\underline{H}_3$), 4.23 (t, 4H, J = 6.7 Hz, $OC\underline{H}_2CH_2$), 4.53–4.62 (m, 4H, CC**H**C), 4.92–4.96 (m, 2H, $CH_2CH{=}C\underline{H}_2$), 4.97–5.04 (m, 2H, $CH_2CH{=}C\underline{H}_2$), 5.82 (ddt, 2H, J = 17.0 Hz, J = 10.3 Hz, J = 6.7 Hz, $CH_2C\underline{H}{=}CH_2$), 6.34 (dd, 2H, J = 8.2 Hz, J = 2.4 Hz, CCHC**H**CO), 6.53 (d, 2H, J = 2.6 Hz, CC**H**CO), 6.82 (d, 2H, J = 8.2 Hz, CC**H**CHCO), 7.00 (d, 2H, J = 7.7 Hz, CC**H**CHCCOOR), 7.55 (dd, 2H, J = 7.7 Hz, J = 1.7 Hz, CCHC**H**CCOOR), 7.60 (d, 2H, J = 1.5 Hz, CC**H**CCOOR); ^{13}C NMR (100 MHz, $CDCl_3$): δ (ppm) = 26.0 (CH_2), 28.7 (CH_2), 28.9 (CH_2), 29.1 (CH_2), 29.3 (CH_2), 29.4 (CH_2), 29.5 (CH_2), 33.8 (CH_2), 52.5 (CH), 53.8 (CH), 55.3 (CH_3), 64.9 (CH_2), 110.6 (CH), 113.5 (CH), 114.1 (CH_2), 127.0 (CH), 127.4 (CH), 127.7 (C), 127.8 (CH), 134.8 (C), 139.2 (CH), 143.7 (C), 144.1 (C), 148.8 (C), 157.8 (C), 166.6 (C); IR ν_{max} cm^{-1}: 2919, 2851, 1705, 1608, 1492, 1437, 1266, 1210, 1162, 1091, 1038; HRMS (m/z for $[M+H]^+$) calcd.: 809.4781; found: 809.4762.

3. Results and discussion

3.1. Synthesis

The followed synthetic pathway of the 2,6-substituted donor-acceptor anthracene derivative first involved the synthesis of a benzyl benzoic acid precursor **6** (Scheme 2, step (i) to (iv)). Ring closure of this compound would result in an anthrone and reduction thereof in an anthracene. First, *m*-anisole (**1**) was brominated using bromine in acetic acid. The resulting 2-bromo-5-methoxybenzaldehyde (**2**) underwent a Grignard reaction using 4-chlorophenylmagnesium bromide (**3**), followed by a reduction to remove the benzylic alcohol group using triethylsilane in trifluoroacetic acid. The resulting bromide of **5** was modified to a carboxylic acid group. This was done by making the Grignard reagent using magnesium, followed by a reaction with anhydrous

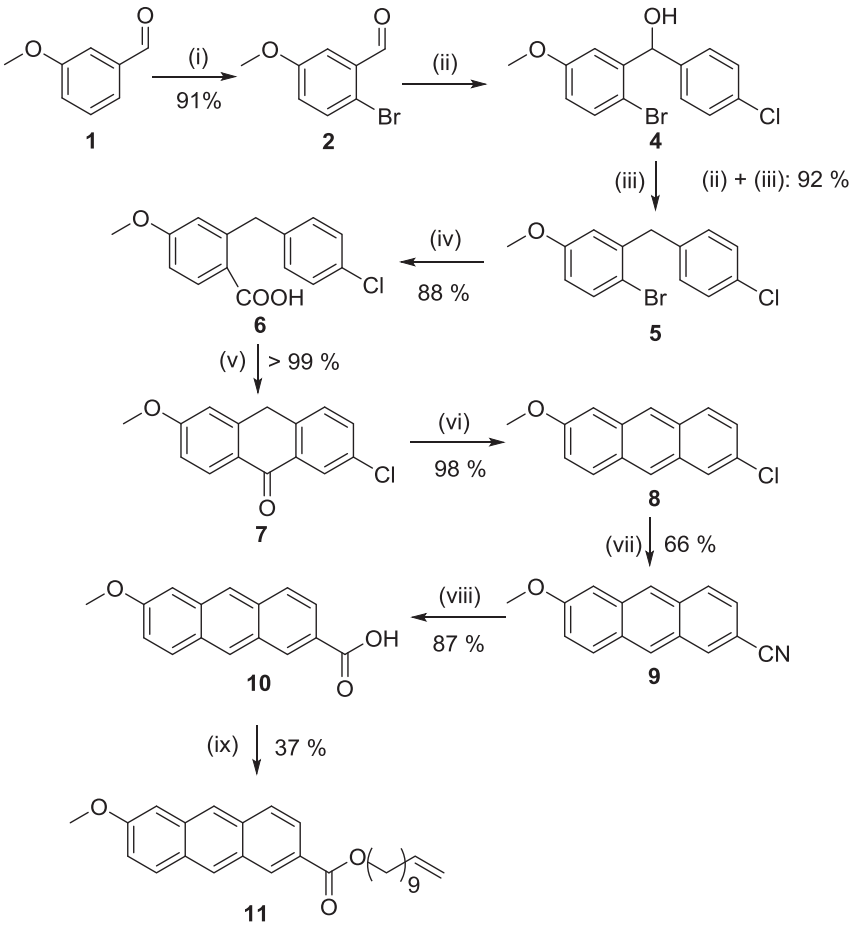

Scheme 2. Synthesis of the anthracene derivatives. (i) Br_2, AcOH, 2 h, rt; 1 h, 70 °C; (ii) (1) 4-chlorophenylmagnesium bromide **3**, diethyl ether, 1 h, rt, (2) H_3O^+; (iii) triethyl silane, trifluoroacetic acid, 18 h, rt; (iv) (1) magnesium, tetrahydrofuran, (2) CO_2, (3) H_3O^+; (v) (1) $SOCl_2$, 2 h, reflux, (2) $AlCl_3$, 1 h, rt; (vi) $NaBH_4$, diglyme, MeOH; (vii) CuCN, NMP, 30 h, reflux; (viii) KOH, H_2O, MeOH, reflux, overnight; (ix) 11-bromo-1-undecene, K_2CO_3, DMF, 24 h, rt.

carbon dioxide. The overall yield for the synthesis of this carboxylic acid was 74%.

Carboxylic acid **6** was then reduced and modified to the desired anthracene (Scheme 2, step (v) to (viii)). Anthrone **7** was made in high yield by first forming the acid chloride from **6** using thionyl chloride, followed by the removal of excess thionyl chloride and ring closure by Friedel-Crafts acylation using aluminum trichloride in dichloromethane. Anthrone **7** was then reduced to anthracene **8** in high yield using sodium borohydride in diglyme. In the absence of a protic solvent, anthracenolate anions are formed, which are unable to reduce to the anthracene or reform the anthrone. Therefore, methanol was added to the solution to allow the kinetically trapped anions to equilibrate with the anthrone, resulting in higher yields [34]. The formed 2-chloro-6-methoxyanthracene **8** was used to make 6-methoxyanthracene-2-carboxylic acid by forming the corresponding Grignard reagent, followed by a reaction with carbon dioxide. However, this proved to be rather difficult. No Grignard reagent formation using magnesium pallets was observed. Attempts to achieve magnesium exchange using isopropylmagnesium chloride lithium chloride complex solution in THF also did not result in any significant end product formation. Only using freshly prepared Rieke magnesium, chloride activation occurred and a yield of 10% carboxylic acid **10** was achieved. This issue with the formation of the Grignard reagent was avoided by synthesizing the nitrile derivative **9** instead. This was done in 66% yield by adding an excess of copper cyanide in *N*-methyl-2-pyrrolidone and heating the solution to reflux for 30 h. The resulting crude 6-methoxyanthracene-2-carbonitrile **9** was easily converted into the desirable 6-methoxyanthracene-2-carboxylic acid **10**. The combined yield over these two steps was 57%, exceeding the results achieved by Grignard reagent formation.

The carboxylic acid functionality of **10** allows making an ester bond linked to a long spacer with a polymerizable end group. The long spacer improves not only the solubility of the anthracene, but also the one of the corresponding dimer. The low solubility of anthracene dimers is often a limiting factor for their use in resin formulations. Therefore, anthracene ester **11**, having better solubility properties, was prepared by performing an addition of the carboxylate anion to 11-bromo-1-undecene in dimethylformamide (Scheme 2, step (ix)). **11** has an end-standing double bond, which can be used either directly as polymerizable groups (*e.g.* for thiol-ene polymerization) or can be modified to acquire other polymerizable functional groups such as oxiranes or alcohols (not done).

3.2. UV–vis absorbance and fluorescence

One of the most important properties of any anthracene derivative, which has to undergo (reversible) dimerization, is their absorption in the UV–visible light spectrum. The absorption spectra of anthracenes **8**, **9**, **10** and **11** were measured in ethanol (Fig. 1 and Table 1).

As expected, two absorption regions can be distinguished for all

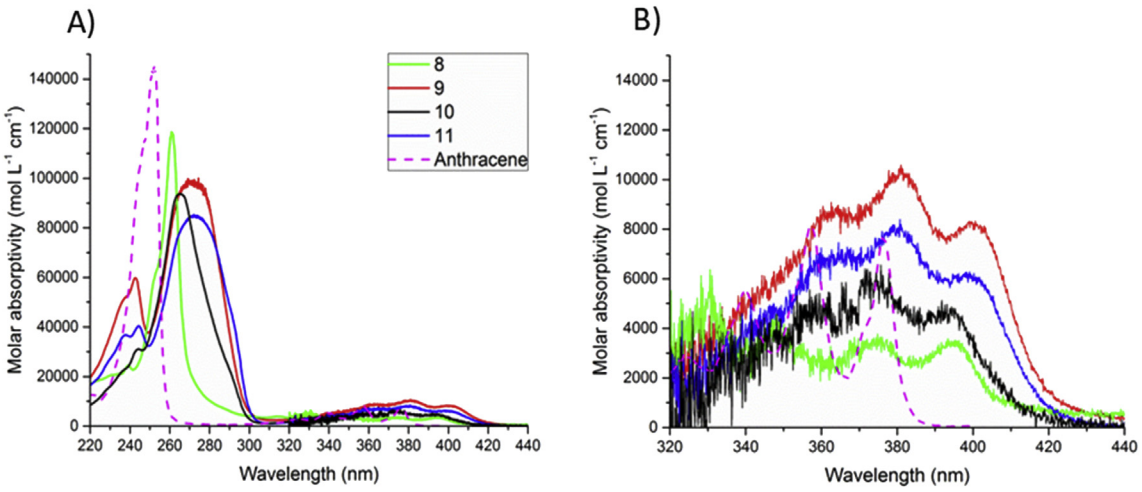

Fig. 1. A) Molar absorptivity of anthracene and four 2,6 derivatives in ethanol B) Zoom in of the region 320–440 nm.

Table 1
Absorption maxima (below and above 300 nm) with molar absorptivity in ethanol. Hammett values σ_p^+ of the 6-substituent, taken from Ref. [35].

	λ_{max} (nm)	ε_{max} (10^3 mol L^{-1} cm^{-1})	λ_{max} (nm)	ε_{max} (10^3 mol L^{-1} cm^{-1})	σ_p^+ of 6-substituent
Anthracene	252	140	357	8.2	–
8	261	120	373	3.5	0.11
9	272	98	381	11	0.66
10	265	94	377	5.6	0.42
11	272	85	380	8.1	0.48

derivatives, one below 300 nm and one above 300 nm. These maxima correspond to respectively longitudinal (long axis) and transversal (short axis) electron density shifts. While excitation using wavelengths from either of these regions may lead to dimerization, in most cases dimerization is performed using only longer wavelengths (>300 nm) to avoid competitive scission. The short wavelength absorption (<300 nm) is red-shifted for all derivatives, compared to unsubstituted anthracene [28,33]. This shift comprises up to 20 nm. By having substituents with a stronger electron withdrawing character (which is identified by having larger Hammett values σ_p^+) in conjugation with the methoxy group, larger red-shifts were achieved. This observation is in accordance to a recent publication based on *in silico* results [36]. While the shape of this absorption peak for **8** is similar to anthracene, it is much broader for the compounds having electron withdrawing groups (**9**, **10** and **11**). This effect is attributed to the higher polarity of the latter compounds, combined with the polar solvent (ethanol), leading to solute-solution interaction. This same interaction also leads to lower molar absorptivity values ε_{max} (Table 1).

The axial absorption (above 300 nm) of the synthesized 2,6-substituted derivatives is also red-shifted up to 24 nm compared to unsubstituted anthracene (Fig. 1B). Again, in combination with the electron donating methoxy group, the conjugated substituents with stronger electron withdrawing properties result in larger red-shifts. The achieved shifts in absorption are higher than previously achieved for 9-substituted anthracenes [28], therefore allowing excitation and subsequent dimerization to occur under milder conditions as we aimed for.

The absorption (Fig. 2A) and fluorescence (Fig. 2B) of anthracene derivative **11** in chloroform, ethanol and acetonitrile were studied to determine possible solvatochromic effects. In both cases, the effects were minor. The emission wavelengths ranged approximately from 400 nm to 600 nm, with peak maxima at 455–460 nm. The emission quantum yields were 0.54 in ethanol and acetonitrile, while being 0.64 in the more apolar chloroform. These high quantum yields suggest a potential use as polymerizable fluorophore.

3.3. Photochemical dimerization

By irradiating a solution of anthracene ester **11** with UVA light, the corresponding photodimers **12** are made. Because of the asymmetric structure of **11**, multiple end products are possible (Fig. 3A). This is also observed in ^{1}H NMR as the different peaks corresponding to the bridge heads around 4.53–4.62 ppm (Fig. 3B). Should only one dimer be formed, 2 doublets of equal integration would have been expected.

The dimerization rate was studied by irradiating 5 and 10 mM solutions of **11** in hexane with UVA light (365 nm, 12 × 9 W), followed by concentration *in vacuo* and quantification via ^{1}H NMR (Fig. 4 and Fig. S31). The dimerization occurred quickly, with 98% conversion reached after 1 h. This is much faster than with the previously studied 9-substituted anthracenes, which under the same conditions only had a conversion of 43–82% after 1 h [28]. The superior dimerization kinetics of **11** is largely due to the absence of steric hindering substituents at the 9- and 10-positions. As a result, not only head-tail but also head-head dimerization can easily occur, which is often not the case for the more commonly used 9-substituted anthracenes.

3.4. UV–vis absorption of dimer 12 and its photochemical scission

Scission of dianthracenes to their parent anthracenes requires excitation by absorption of photons. As can be seen in Fig. 5A, dimers **12** have a red-shifted absorption, with a large shoulder peak at 232 nm. This red-shift is a result of the position of the substituents, which after dimerization are directly connected to the benzene rings of the dimer structure. This is not the case for 9-

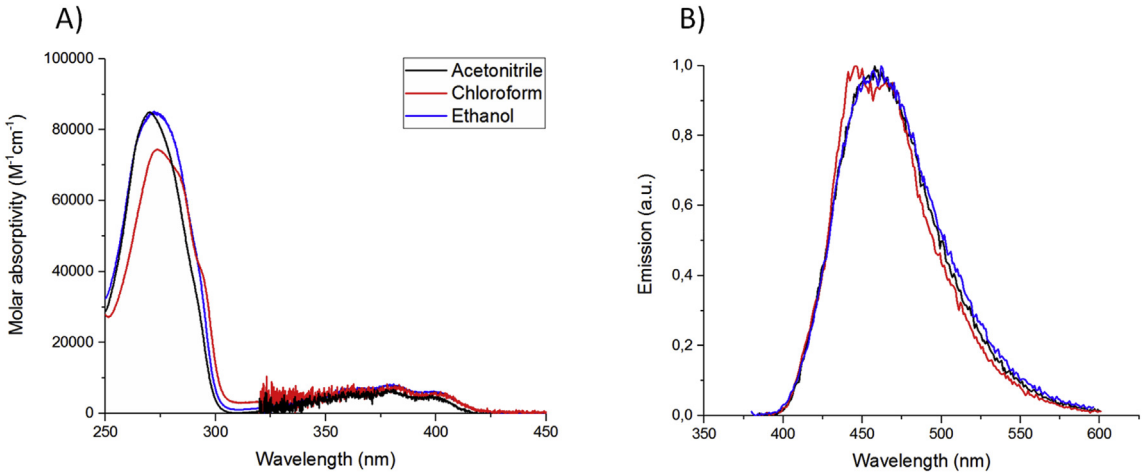

Fig. 2. Molar absorptivity (A) and emission after excitation at absorption peak maximum (interval 300–420 nm) (B) of **11** in acetonitrile, chloroform and ethanol.

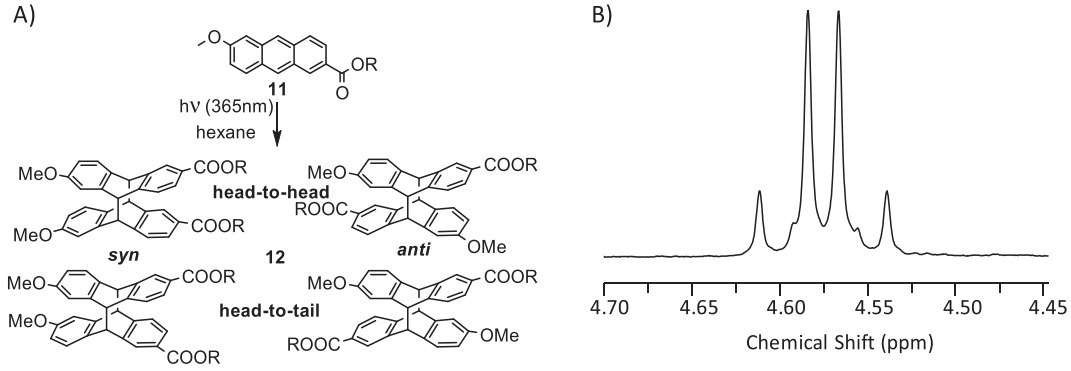

Fig. 3. (A) Possible photodimerization products **12** obtained from anthracene ester **11;** (B) Zoom of the ^{1}H NMR spectrum of photodimers **12**. The peaks originate from the anthracene dimer bridge heads.

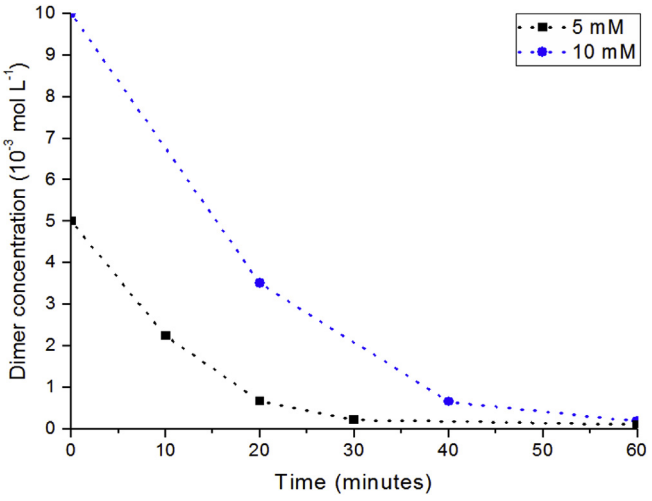

Fig. 4. Photodimerization (365 nm; 12 × 9 W) of **11** in hexane.

substituted anthracenes, which after dimerization no longer have the substituent being part of an aromatic system.

Photochemical scission of **12** and dianthracene was studied by observing the appearance of the UV–vis absorption peak of **11** as a function of irradiation time (270 nm and 252 nm) (Fig. 5B). The samples were irradiated using 11 lamps of 254 nm (9 W each). It should be noted that for analytical reasons each 5 s interval included starting the UV-lamps. Therefore, the actual irradiation time is lower and the dimerization actually occurs faster upon continuous irradiation. The measured absorptions A were normalized to the maximum absorption achieved for each sample A_{max}. From Fig. 5B, it is clear that the photochemical scission of **12** occurs much faster than for unsubstituted anthracene. In fact, scission of **12** reached its maximum after only 15 s, while for dianthracene the maximum was only achieved after 2 min. These superior properties are the result of the achieved absorption red-shifts by substitution on the 2- and 6- positions. Indeed, not only does **12** absorb more light at 254 nm than dianthracene, but the resulting compound **11** also absorbs less of these wavelengths than the unsubstituted anthracene.

3.5. Thermal scission in bulk and in solution

The thermal scission of dimers **12** was studied in a solution of a high boiling point solvent (tributyrin). The concentration of **11** produced by thermal scission was quantified by measuring the fluorescence of **11** in the samples taken every few minutes. Conversions were normalized to the last sample taken. By plotting the acquired rate constants k at different temperatures, the Arrhenius plot could be obtained from which the Arrhenius parameters can be derived (Fig. 6A). The derived activation energy E is 156.4 kJ mol^{-1} with a pre-exponential factor A_{exp} of 8.7 10^{14} s^{-1}. This thermal

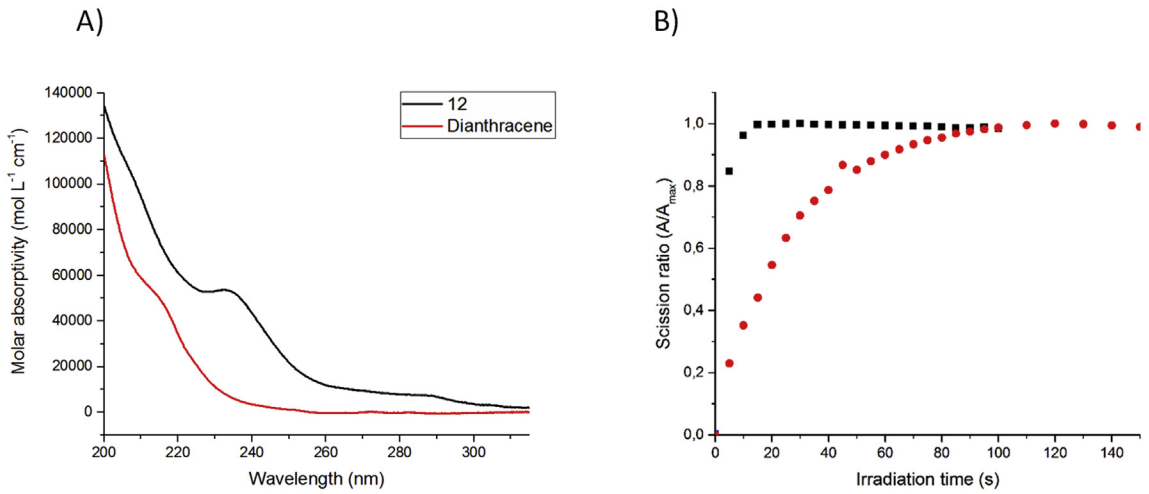

Fig. 5. UV–vis absorption spectra (A) and Photoscission (254 nm) of 2.8 μM solutions (B) of the photodimers **12** and unsubstituted dianthracene in acetonitrile.

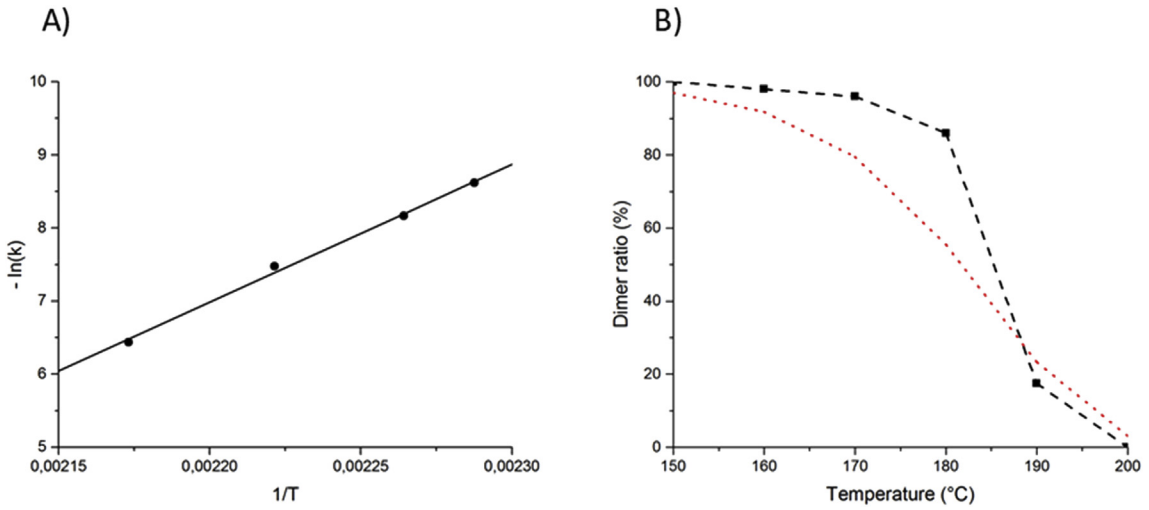

Fig. 6. (A) Arrhenius plot of the thermal scission of **12**; (B) Thermal scission of **12** in bulk, determined using 1H NMR, after controlled heating (10 K min-1) and a 10 min isothermal step. Black squares: experimental data; red dotted line: estimated conversion.

stability is slightly higher than what was previously reported for a 9-anthracene methanol based derivative (Supporting Information, Table S1) [29].

The thermal scission in bulk was studied by ^{1}H NMR measurements after controlled heating and an isothermal step of 10 min in a DSC apparatus. The results thereof are shown in Fig. 6B and Fig. S2 (Supporting information). These figures show that significant scission only occurs after heating for 10 min at 180 °C or higher temperatures. Calculations using the determined Arrhenius parameters from solution, estimated much lower dimer ratios at 180 °C and lower temperatures. This mismatch between the estimated ratios and the experimental data from bulk is ascribed to the high melting point of **12** (198 °C). The stabilizing effect of the dimer crystal lattice initially slows down the thermal dissociation [28,37]. A complex thermal behavior is expected by the superposition of thermal dissociation and melting of the dimer. Presumably some thermal scission takes place, resulting in liquid **11**, which dissolves remaining dimer. Nevertheless, this high melting point means that at 180 °C and lower, **12** must have been crystalline, leading to a much slower thermal scission.

4. Conclusion

A soluble, functional 2,6 donor-acceptor anthracene derivative and its photochemically obtained dimer were successfully synthesized from readily available compounds. By using stronger electron withdrawing groups, in combination with the donating methoxy group, larger absorption red-shifts were achieved. This was observed for both the axial (above 300 nm) and longitudinal (below 300 nm) absorptions. In addition, the high fluorescence quantum yield (0.54–0.64) also allowed its use as efficient fluorophore. As there are no substituents present on the middle ring, dimerization occurred much faster than for commonly used 9-substituted anthracenes. Furthermore, because of the absorption red-shifts for both monomer and dimers, the compound also exhibited superior photoscission properties. Finally, thermal scission occurred cleanly, but required high temperatures (>180 °C). This is especially true in bulk, where crystallization increased the thermal stability even more. The high thermal stability of this dianthracene allows its use in high temperature short-term and low temperature long-term applications, while the high photoreactivity allows fast changes in cross-link density.

The use of longer substituent chains [28] and the incorporation into (densely) crosslinked polymer networks [29] are known to reduce the crystallization of the anthracene dimers and monomers. A further change of the nature of the 2,6-substituents would allow for the preparation of stimuli-responsive polymers with tailored thermal and photochemical responsiveness that could prove especially useful for applications such as reversible adhesion, stress-relaxation and self-healing materials.

Acknowledgements

This work was supported by FWO-Vlaanderen (Project G006913N). J.V.D. acknowledges Flanders Innovation & Entrepreneurship (VLAIO) for financial support.

Appendix A. Supplementary data

Supplementary data to this article can be found online at https://doi.org/10.1016/j.tet.2019.01.007.

References

[1] H. Bouas-Laurent, A. Castellan, J.-P. Desvergne, R. Lapouyade, Chem. Soc. Rev. 29 (2000) 43–55.
[2] H. Bouas-Laurent, A. Castellan, J.-P. Desvergne, R. Lapouyade, Chem. Soc. Rev. 30 (2001) 248–263.
[3] P. Zhao, C.F. Fang, C.J. Xia, Y.M. Wang, D.S. Liu, S.J. Xie, Appl. Phys. Lett. 93 (2008), 013113.
[4] E.M. Nofen, J. Wickham, B. Koo, A. Chattopadhyay, L.L. Dai, Mater. Res. Express 3 (2016).
[5] Z. Gao, Y. Han, F. Wang, Nat. Commun. 9 (2018) 3977.
[6] G. McSkimming, J.H.R. Tucker, H. Bouas-Laurent, J.P. Desvergne, Angew. Chem. Int. Ed. 39 (2000) 2167–2169.
[7] H. Bouas-Laurent, A. Castellan, J.-P. Desvergne, Pure Appl. Chem. (1980) 2633.
[8] C.J. Kloxin, C.N. Bowman, Chem. Soc. Rev. 42 (2013) 7161–7173.
[9] C.J. Kloxin, T.F. Scott, B.J. Adzima, C.N. Bowman, Macromolecules 43 (2010) 2643–2653.
[10] W. Denissen, J.M. Winne, F.E. Du Prez, Chem. Sci. 7 (2016) 30–38.
[11] Y. Zhang, A.A. Broekhuis, F. Picchioni, Macromolecules 42 (2009) 1906–1912.
[12] S. Burattini, B.W. Greenland, D. Chappell, H.M. Colquhoun, W. Hayes, Chem. Soc. Rev. 39 (2010) 1973–1985.
[13] S.D. Bergman, F. Wudl, J. Mater. Chem. 18 (2008) 41–62.
[14] T. Maeda, H. Otsuka, A. Takahara, Prog. Polym. Sci. 34 (2009) 581–604.
[15] Y.-L. Liu, T.-W. Chuo, Polym. Chem. 4 (2013) 2194–2205.
[16] A. Gandini, Prog. Polym. Sci. 38 (2013) 1–29.
[17] G. Kaur, P. Johnston, K. Saito, Polym. Chem. 5 (2014) 2171–2186.
[18] W.D. Cook, F. Chen, Q.D. Nghiem, T.F. Scott, C.N. Bowman, S. Chausson, L. Le Pluart, Macromol. Symp. 291–292 (2010) 50–65.
[19] R.-C. Brachvogel, M. von Delius, Eur. J. Org. Chem. 2016 (2016) 3662–3670.
[20] R. Nicolaÿ, J. Kamada, A. Van Wassen, K. Matyjaszewski, Macromolecules 43 (2010) 4355–4361.
[21] N. Roy, J.-M. Lehn, Chem. Asian J. 6 (2011) 2419–2425.
[22] A.M. Schenzel, N. Moszner, C. Barner-Kowollik, Polym. Chem. 8 (2017) 414–420.
[23] T. Zdobinsky, P. Sankar Maiti, R. Klajn, J. Am. Chem. Soc. 136 (2014) 2711–2714.
[24] J. Van Damme, F. Du Prez, Prog. Polym. Sci. 82 (2018) 92–119.
[25] P. Froimowicz, H. Frey, K. Landfester, Macromol. Rapid Commun. 32 (2011) 468–473.
[26] Y. Sako, Y. Takaguchi, Org. Biomol. Chem. 6 (2008) 3843–3847.
[27] A. Sanyal, Q. Yuan, J.K. Snyder, Tetrahedron Lett. 46 (2005) 2475–2478.
[28] J. Van Damme, L. Vlaminck, G. Van Assche, B. Van Mele, O. van den Berg, F. Du Prez, Tetrahedron 72 (2016) 4303–4311.
[29] J. Van Damme, O. van den Berg, J. Brancart, L. Vlaminck, C. Huyck, G. Van Assche, B. Van Mele, F. Du Prez, Macromolecules 50 (2017) 1930–1938.
[30] T.K. Claus, S. Telitel, A. Welle, M. Bastmeyer, A.P. Vogt, G. Delaittre, C. Barner-Kowollik, Chem. Commun. 53 (2017) 1599–1602.
[31] T. Yamamoto, S. Yagyu, Y. Tezuka, J. Am. Chem. Soc. 138 (2016) 3904–3911.
[32] Z. Lu, S.J. Lord, H. Wang, W.E. Moerner, R.J. Twieg, J. Org. Chem. 71 (2006) 9651–9657.
[33] H. Ihmels, Eur. J. Org. Chem. 1999 (1999) 1595–1600.
[34] D.J. Marquardt, F.A. McCormick, Tetrahedron Lett. 35 (1994) 1131–1134.
[35] C. Hansch, A. Leo, R.W. Taft, Chem. Rev. 91 (1991) 165–195.
[36] S. Abou-Hatab, V.A. Spata, S.J. Matsika, Phys. Chem. A 121 (2017) 1213–1222.
[37] D. Donati, G. Guarini, P. Sarti-fantoni, Mol. Cryst. Liq. Cryst. 17 (1972) 187–195.